

**INTERPRETING MAGNETIC ANOMALY SIGNATURES OBSERVED OVER THE NEARSIDE LUNAR MARE BASINS.** K. Hemant<sup>1</sup>, M. E. Purucker<sup>2</sup> and T. J. Sabaka<sup>2</sup>, <sup>1</sup>ORAU at Planetary Geodynamics Lab, GSFC (Code 698, GSFC/NASA, Greenbelt, MD 20771, [hemant@puuoo.gsfc.nasa.gov](mailto:hemant@puuoo.gsfc.nasa.gov)), <sup>2</sup>Ratheyon at Planetary Geodynamics Lab, GSFC (Code 698, GSFC/NASA, Greenbelt, MD 20771, [purucker@puuoo.gsfc.nasa.gov](mailto:purucker@puuoo.gsfc.nasa.gov), [sabaka@geomag.gsfc.nasa.gov](mailto:sabaka@geomag.gsfc.nasa.gov)).

**Introduction:** The lunar-wide magnetic anomaly map derived from Lunar Prospector (LP) magnetometer (MAG) data [1] now allows for interpreting the anomalies in terms of structure, composition and direction of magnetization. The lunar crustal thickness model, paleomagnetic measurements from the Apollo samples [2] and the geologic map of the nearside of the Moon [3] are combined together on a Geographic Information System (GIS) to compute a lunar crustal magnetization model. Magnetic anomaly map is calculated and compared with the corresponding observed magnetic anomaly map. The source distribution causing the observed anomalies over the nearside lunar mare basins are interpreted in terms of thicknesses of the underlying mare basalts.

**New magnetic map:** The mare basalts have been sampled and returned by Apollo and Soviet Luna missions. They have been sampled from widely separated locations on the lunar nearside (Apollo 11, 12, 15, 17 and Luna 16). Eruptions of these mare basalts are contemporaneous with extensive mare volcanism that filled the great basins [4, 5, 6]. The Clementine and LP missions provided compositional and magnetometer data that is used to identify mare basalts composition on the Moon and their associated magnetic signatures. The magnetic anomaly map derived from low-altitude period of the LP mission extends up to spherical harmonic degree 150 and is now available for interpretation (Fig. 1a). The resolution of MAG data is 0.5 degree in latitude and 1.0 degree in longitude.

The radial component ( $B_r$ ) of the MAG model show weak anomalies over the lunar mare basins and strong anomalies over the regions diametrically opposite to the largest basin-forming impact craters (Fig. 1a). Conversely, the spectrometer data over the Lunar mare regions show a high concentration of FeO by weight [7], suggesting iron could mostly be present in the form of ilmenites and other high Titanium oxide not producing magnetic anomalies observable at satellite altitude of 30 km. Among the mare basins, Crisium and Marginis show amplitudes  $> 4$  nT at 30 km altitude while Serenitatis, Fecundiatis, Nectaris, Australe and Moscoviense basins show strength  $< 4$  nT. Large mare basins Imbrium and Orientale show the weakest features  $< 1.5$  nT within the basin, but often the strength exceeds  $> 2.0$  nT southwest of the basin.

**Magnetic field modeling:** The geological map showing distribution of mare filled basins on the nearside is modeled by assuming an average composition of natural remanent magnetization (NRM) of the Apollo samples. The top 20-30 m of regolith soils are underlain by varying thickness of 1-2 km thick of mare basalts. Much of the upper crust is considered noritic with thickness of 10-15 km while mid to lower crust is assumed to non-magnetic anorthosite. Rest of the lower crust is considered to be basalts whose thicknesses could be varying significantly based on the thickness of crust within mare basins. The derived vertically integrated magnetization (VIM) model is shown in Figure 1b. VIM model for lunar highland is computed using the 2-layered crustal thickness model of Wieczorek et al. [8] obtained from inversion of LP gravity data. The direction of magnetization is assumed to follow a paleo-magnetic field computed using the intensity of the magnetic field obtained from Apollo samples [2]. Changes in magnetization direction due to the impact of small and large projectiles has not been modeled here and hence are not used to interpret observed anomaly features. The calculated magnetic anomalies for the  $B_r$  component is calculated from this VIM model and is shown over the nearside lunar mare basins (Fig. 1c). The calculated anomaly is predicted at 30 km altitude and extends up to spherical harmonic degree 150.

**Discussion:** The match between the field predicted from lunar surface geology and the observed field is in agreement in terms of amplitude of anomaly features over the nearside lunar mare basins. Anomalies over the central Mare Imbrium, Mare Crisium, Mare Marginis and lunar highland regions between Mare Nubium and Mare Nectaris are however poorly-defined in the predicted map (Fig. 1). The moderately high over the Mare Serenitatis and Mare Nectaris is not reproduced in the calculated field. Some of the weak anomaly features over the Mare Humboldtianum, Mare Symthii, Mare Humorom and west of Mare Cognitum agree well with observations although spatial distribution of anomalies do not match completely.

The results from the preliminary magnetic field modeling suggest that the 1-2 km thickness of the Mare basalts are possible sources contributing to the observed magnetic anomalies within the lunar crust. However constrains from LP and Clementine spectral

maps can be used to adjust the spatial distribution of the inferred rock types in the VIM model. In addition, the magnetization direction modified due to shock imparted by large impact should be included to model the modified source distribution within the impact basins [9]. Forward modeling approach such as implemented above offers greater flexibility in designing crustal magnetization models based on rock type information, rock magnetic properties and crustal structure within a lunar geologic regime. Such forward models lead to predicted magnetic field models which can be modified with ease based on information obtained from other geophysical experiments.

**References:** [1] Purucker, M.E. (2008) (in press) *Icarus*. [2] Fuller, M. and Cisowski, S.M. (1987) In: *Geomagnetism*, vol. 2, 307-456. [3] Wilhelms, D.E. (1971) [file:///C:/Moon/geology/10703/10703\\_g.htm](file:///C:/Moon/geology/10703/10703_g.htm). [4] Dasch, E. J. et al. (1987) *Geochim. Cosmochim. Acta*, 51, 3241-54. [5]. Nyquist, L.E. and Shih, C.Y. (1992), *Geochim. Cosmochim. Acta*, 56, 2213-34. [6] Synder, G.A. et al. (2000) In: *Origin of Earth and Moon*, 361-395. [7] Lucey, P.G. et al. (1995) *Science*, 268, 1150-1153. [8] Wieczorek et al. (2006) *Rev. Mineral. Geochem.*, 60, 221-364. [9] Cisowski, S.M. et al. (1975) *Geochim. Cosmochim. Acta*, 39, 3123-41.

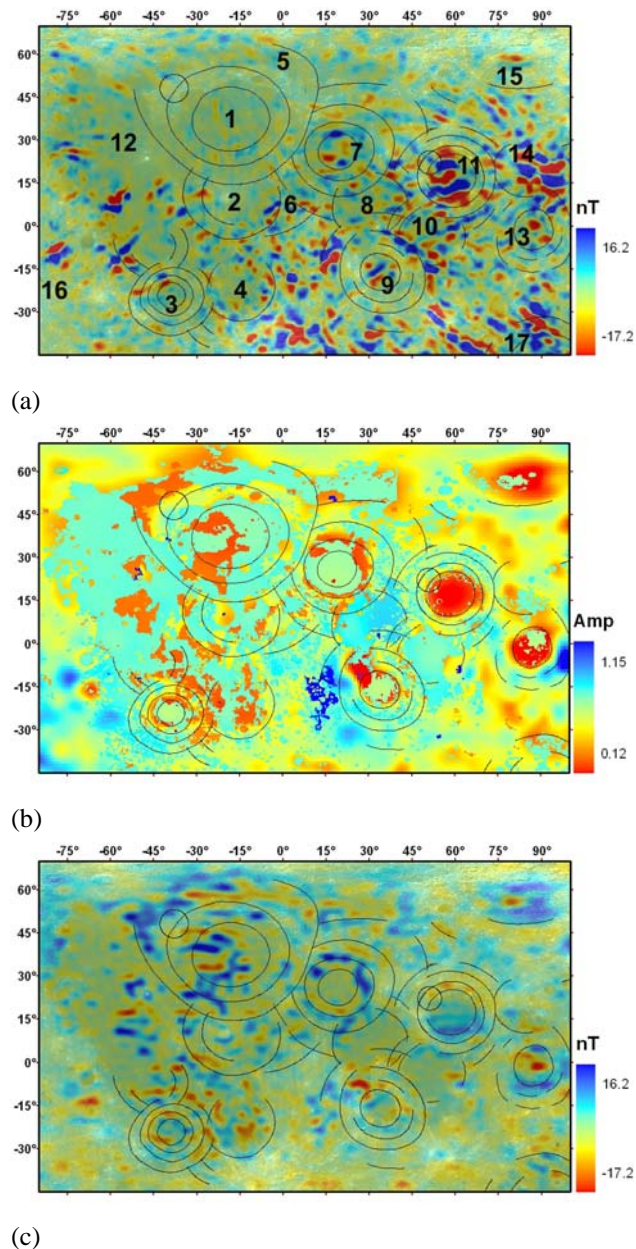


Figure 1. a)  $B_r$  component of magnetic field measured by Magnetometer (MAG) after [1] shown over Lunar Mare basins. The numbers denote the large impact basins: 1. Mare Imbrium, 2. Mare Cognitum, 3. Mare Humorum, 4. Mare Nubium, 5. Mare Frigoris, 6. Mare Vaporum, 7. Mare Serenitatis, 8. Mare Tranquillitatis, 9. Mare Nectaris, 10. Mare Fecunditatis, 11. Mare Crisium, 12. Mare Oceanus Procellarum, 13. Mare Smythii, 14. Mare Marginis, 15. Mare Humboldtianum, 16. Mare Orientale, 17. Mare Australe. b) Vertically integrated magnetization model of the nearside Lunar Mare basins. c)  $B_r$  component of the calculated magnetic anomaly from VIM model shown in (a).